

## Optimal Power Flow for Distribution Networks with Distributed Generation

Jordan Radosavljević<sup>1</sup>, Miroslav Jevtic<sup>1</sup>,  
Dardan Klimenta<sup>1</sup>, Nebojša Arsić<sup>1</sup>

**Abstract:** This paper presents a genetic algorithm (GA) based approach for the solution of the optimal power flow (OPF) in distribution networks with distributed generation (DG) units, including fuel cells, micro turbines, diesel generators, photovoltaic systems and wind turbines. The OPF is formulated as a nonlinear multi-objective optimization problem with equality and inequality constraints. Due to the stochastic nature of energy produced from renewable sources, i.e. wind turbines and photovoltaic systems, as well as load uncertainties, a probabilistic algorithm is introduced in the OPF analysis. The Weibull and normal distributions are employed to model the input random variables, namely the wind speed, solar irradiance and load power. The 2m+1 point estimate method and the Gram Charlier expansion theory are used to obtain the statistical moments and the probability density functions (PDFs) of the OPF results. The proposed approach is examined and tested on a modified IEEE 34 node test feeder with integrated five different DG units. The obtained results prove the efficiency of the proposed approach to solve both deterministic and probabilistic OPF problems for different forms of the multi-objective function. As such, it can serve as a useful decision-making supporting tool for distribution network operators.

**Keywords:** Optimal power flow, Distribution network, Distributed generation, Genetic algorithm, Point estimate method.

### 1 Introduction

Electricity distribution companies tend to integrate different types of distributed generation (DG) units in the distribution network [1]. Integration of DG units with renewable energy such as photovoltaic (*pv*) systems, small wind turbines (*wt<sub>s</sub>*) and small hydro power plants is influenced by geographical and meteorological conditions. The DG units with non renewable energy, including fuel cells (*fc<sub>s</sub>*), micro turbines (*mt<sub>s</sub>*) and diesel generators (*dg<sub>s</sub>*), can be connected to any point of the distribution network, but the fuel cost must be

---

<sup>1</sup>Faculty of Technical Sciences, University of Priština in Kosovska Mitrovica, Kneza Miloša 7, 38220 Kosovska Mitrovica, Serbia; E-mails: jordan.radosavljevic@pr.ac.rs; mirolub.jevtic@pr.ac.rs; dklimenta@hotmail.com; nebojsa.arsic@pr.ac.rs

taken into account. Depending on the DG units technologies, the primary energy of DG units may be injected into the distribution network via either a synchronous or asynchronous electric machine which is directly connected to the grid, a combination of an electric machine and a power electronic interface, or only via a power electronic interface. If electric machine is directly connected to the grid, its operation determines the model of DG unit (PQ or PV node) for power flow studies. In other cases, the characteristics of the interface control circuit determine the DG unit model. As a general rule, in case when the control circuit of the converter is designed to control active power and voltage independently, the DG unit model shall be as a PV node and when it is designed to control active and reactive power independently, the DG unit model shall be as a PQ node [2].

Generally, DG units, if properly planned and controlled, may offer improved voltage profile and power losses reduction of the distribution network, better economics and a reduced dependence on the local utility [3]. The benefits can be achieved only through efficient coordination of the DG units operation, voltage regulation (voltage regulators, ULTC) and reactive power compensation (VAR compensators) within the distribution network. In fact, it is an optimal power flow (OPF) problem.

Main objective of the OPF for a distribution network is to minimize the fuel cost of DG units [4,5], voltage profile improvement [6] and minimization of power losses [7,8], though optimal settings of the control variables, while at the same time satisfying various distribution system operating constraints. In [4], an optimal distribution power flow strategy based on decomposition of the overall system problem into two components: economic dispatch for energy at the system level and loss minimization at the distribution level is proposed. A generalized formulation to determine the optimal operating strategy and cost optimization scheme for a microgrid consist of a *wt*, a *mt*, a *dg*, a *pv* array, a *fc*, and a battery storage has been presented in [5]. In this strategy, the mesh adaptive direct search algorithm is used to minimize the cost function of the system while constraining it to meet the customer demand and safety of the system. Other objectives, such as power loss minimization and voltage profile improvement, as well as power flow constraints and bus voltage constraints are not considered. In [9], combined problem formulation for active-reactive OPF in distribution networks with embedded wind generation and battery storage is proposed. Ref. [10] proposed a mixed integer linear programming model for volt/var optimization in distribution feeders and analyzes its characteristics and performances by means the application to different test feeders in various operating conditions. In these papers, the uncertainties of the input variables such as power load and power generation from renewable DG units are not considered. These deterministic approaches are highly dependent on the

accuracy of the input data. When some of the input variables are uncertain, the OPF should be treated as a probabilistic problem.

It is well known that the load forecast is always subject to certain errors. In [11], the uncertainty of undetermined load is modeled by normal distribution and OPF problem is defined with several constraints. An OPF with multiple data uncertainties, including load forecast, constraints' limits and cost curve coefficients have been presented in [12]. Moreover, because of the probabilistic nature of the wind speed and solar irradiance, the wind and solar units generate random and fluctuated power. A probabilistic approach for the energy and operation management of renewable microgrids under uncertain environment has been proposed in [13]. The Weibul distribution for wind speed and normal PDF for loads is assumed in [14] to investigate the probabilistic OPF problem by applying the point estimate method. In [15], stochastic behavior of market participants is introduced in the OPF calculation by means of a two-point estimate method.

The main purpose of this paper is the development of a generalized approach for the OPF analysis in distribution networks. Among other, this implies the inclusion of different types of DG units, taking into account the uncertainties of the input variables, the multi-objective optimization and choice of an efficient method for solving the OPF.

In Section 2, we formulated the deterministic OPF as a nonlinear multi-objective optimization problem with equality and inequality constraints. This formulation includes the DG units with renewable and non-renewable energy sources. Optimization models of the DG units are given in Section 3. In this paper, the GA has been used to solve the OPF problem. The GA, as an intelligent and widely used heuristic optimization algorithm, is briefly described in Section 4. In addition to the deterministic, a probabilistic OPF algorithm based on the  $2m+1$  point estimate method is presented in Section 5. The Weibull and normal distributions are employed to model the input random variables, namely the wind speed, solar irradiance and load power. The Gram Charlier expansion series are used to obtain PDFs of the OPF results. The proposed approach is tested on a modified IEEE 34 node test feeder. The following objective functions are considered: (i) fuel cost minimization for DG units (ii) simultaneous minimization of the fuel cost and power losses (iii) simultaneous minimization of the fuel cost and voltage deviation and (iv) simultaneous minimization of the fuel cost, power losses and voltage deviation. Section 6 presents the results of simulation. Finally, the main contributions of this paper are summarized in Section 7.

## 2 Deterministic Optimal Power Flow

The goal of the OPF is to minimize a selected objective function via optimal settings of the control variables, subjected to various equality and inequality constraints. Generally, the OPF problem can be formulated as follows [16 – 21]:

$$\min F(x, u), \quad (1)$$

$$\text{Subject to: } g(x, u) = 0, \quad (2)$$

$$h(x, u) \leq 0, \quad (3)$$

$$u \in U, \quad (4)$$

where  $F$  is the objective function to be minimized,  $x$  and  $u$  are vectors of dependent and control variables, respectively.

For a distribution networks, the vector of dependent variables ( $x$ ) consisting of:

- The active power from the electric grid  $P_{gr}$ ;
- Load node voltages, including DG units which are modeled as PQ nodes,  $V_L$ ;
- The reactive power outputs of the DG units which are modeled as PV nodes  $Q_{DG}$ ;
- Branch flows  $S_l$ .

Therefore,  $x$  can be expressed as:

$$x = [P_{gr}, V_{L1} \dots V_{LN}, Q_{DG1} \dots Q_{DGNPV}, S_{I1} \dots S_{IN}]^T, \quad (5)$$

where  $NL$ ,  $NPV$  and  $N$  are the number of load nodes, number of PV nodes, and number of nodes (namely branches) in the distribution network, respectively.

Vector of control variables ( $u$ ) consisting of:

- The active power outputs of the DG units with nonrenewable energy sources  $P_{DG}$ ;
- Root node voltage  $V_0$ ;
- The terminal voltages at PV nodes  $V_{PV}$ ;
- Transformer (voltage regulation) tap settings  $t$ ;
- The outputs of shunt VAR compensators  $Q_C$ .

Therefore, the vector of control variables can be expressed as:

$$u = [P_{DG1} \dots P_{DGNNR}, V_0, V_{PV1} \dots V_{PVNPV}, t_1 \dots t_{NT}, Q_{C1} \dots Q_{CNC}]^T, \quad (6)$$

where  $NNR$ ,  $NPV$ ,  $NT$  and  $NC$  are number of the nonrenewable DG units, number of PV nodes (DG units modeled as PV nodes), number of regulating transformers, and number of VAR compensators, respectively.

## 2.1 Objective Function

The objective function can take different forms. Several cases have been considered in this paper.

**Case 1:** Fuel cost minimization.

$$F = f_{gr}(P_{gr}) + \sum_{i=1}^{NNR} f_i(P_{DGi}), \quad (7)$$

where  $f_{gr}(P_{gr})$  and  $f_i(P_{DGi})$  are the electric grid and DG units cost characteristics, respectively.

**Case 2:** Multi-objective OPF as simultaneous minimization of the fuel cost and power losses:

$$F = f_{gr}(P_{gr}) + \sum_{i=1}^{NNR} f_i(P_{DGi}) + w_{Ploss} \sum_{i=1}^N Ploss_i, \quad (8)$$

where  $Ploss_i$  and  $w_{Ploss}$  are the power loss in branch  $i$  and weighting factor for power losses, respectively.

**Case 3:** Multi-objective OPF as simultaneous minimization of the fuel cost and voltage deviation at load nodes:

$$F = f_{gr}(P_{gr}) + \sum_{i=1}^{NNR} f_i(P_{DGi}) + w_v \sum_{i=1}^{NL} |1 - V_i|, \quad (9)$$

where  $V_i$  and  $w_v$  are the voltage magnitude at load node  $i$  and weighting factor for voltage deviation, respectively.

**Case 4:** Multi-objective OPF as simultaneous minimization of the fuel cost, power losses and voltage deviation at load nodes:

$$F = f_{gr}(P_{gr}) + \sum_{i=1}^{NNR} f_i(P_{DGi}) + w_{Ploss} \sum_{i=1}^N Ploss_i + w_v \sum_{i=1}^{NL} |1 - V_i|. \quad (10)$$

## 2.2 Constraints

The equality constraints (2) represent typical power balance and power flow equations. The power balance equation in distribution network with DG units with renewable and nonrenewable energy sources can be expressed as follows:

$$\sum_{i=1}^{NNR} P_{DGi} + P_{gr} = \sum_{i=1}^{NL} P_{Li} + \sum_{i=1}^N Ploss_i - \sum_{i=1}^{NR} P_{DGi}, \quad (11)$$

where  $NR$  is number of DG units with renewable energy sources.

The backward/forward sweep power flow equations are given in [22, 23].

Inequality constraints (3) are the functional operating constraints containing: load bus voltage magnitude limits, DG units reactive power capabilities and branch flow limits:

$$V_i^{\min} \leq V_i \leq V_i^{\max}, \quad i = 1, \dots, NL, \quad (12)$$

$$Q_{DGi}^{\min} \leq Q_{DGi} \leq Q_{DGi}^{\max}, \quad i = 1, \dots, NPV, \quad (13)$$

$$S_i \leq S_i^{\max}, \quad i = 1, \dots, N. \quad (14)$$

Constraints (4) define the feasibility region of the problem control variables such as: DG unit active power output limits, root node voltage magnitude limits, PV node voltage magnitude limits, transformer tap setting limits and shunt VAR compensation limits:

$$P_{DGi}^{\min} \leq P_{DGi} \leq P_{DGi}^{\max}, \quad i = 1, \dots, NNR, \quad (15)$$

$$V_0^{\min} \leq V_0 \leq V_0^{\max}, \quad (16)$$

$$V_{DGi}^{\min} \leq V_{DGi} \leq V_{DGi}^{\max}, \quad i = 1, \dots, NPV, \quad (17)$$

$$t_i^{\min} \leq t_i \leq t_i^{\max}, \quad i = 1, \dots, NT, \quad (18)$$

$$Q_{Ci}^{\min} \leq Q_{Ci} \leq Q_{Ci}^{\max}, \quad i = 1, \dots, NC. \quad (19)$$

Inequality constraints of the dependent variables contain load bus voltage magnitudes, DG units reactive power outputs and branch loadings is added to the objective function as a quadratic penalty terms [16]. The new expanded objective function to be minimized becomes:

$$F_p = F + \lambda_V \sum_{i=1}^{NL} (V_i - V_i^{\lim})^2 + \lambda_{QDG} \sum_{i=1}^{NPV} (Q_{DGi} - Q_{DGi}^{\lim})^2 + \lambda_S \sum_{i=1}^N (S_i - S_i^{\lim})^2, \quad (20)$$

where  $\lambda_V$ ,  $\lambda_{QDG}$  and  $\lambda_S$  are defined as penalty factors.  $x^{\lim}$  is the limit value of the dependent variable  $x$  and given as [21]:

$$x^{\lim} = x^{\max} \quad \text{if } x > x^{\max} \quad \text{and} \quad x^{\lim} = x^{\min} \quad \text{if } x < x^{\min}. \quad (21)$$

### 3 DG Units Modeling For Optimal Power Flow

#### 3.1 Diesel generator

Usually, the diesel fuel consumption data in (L/h) at 25%, 50%, 70% and 100% of the diesel generator power rating (kW) are given by the manufacturer. Based on these data, the fuel consumption characteristic of the diesel generator can be estimated as a quadratic function of its active power output:

$$Fuel_{dg} = a + bP_{dg} + cP_{dg}^2, \quad (22)$$

where  $Fuel_{dg}$  is the diesel generator fuel consumption in (L/h),  $P_{dg}$  is the diesel generator power output in (kW),  $a$ ,  $b$  and  $c$  are coefficients of the fuel consumption characteristic. Accordingly, the total (\$/h) diesel generator fuel cost  $f_{dg}$  can be calculated as:

$$f_{dg} = c_{dg} Fuel_{dg} = c_{dg} (a + bP_{dg} + cP_{dg}^2), \quad (23)$$

where  $c_{dg}$  is the diesel fuel price to supply the diesel generator in (\$/L). We assume that MDJW 410 T6, 369 kW diesel generator is used in this paper. The diesel fuel consumption data of the diesel generator is available in [24]. Based on these data and the fuel price was adopted  $c_{dg} = 0.6$  (\$/L), we obtain the fuel costs characteristic shown in Fig. 1.

### 3.2 Fuel cell

Fuel cost for the fuel cell is dependent of the active power output and the fuel cell efficiency [5, 25]:

$$f_{fc} = c_{fc} P_{fc} / \eta_{fc}, \quad (24)$$

where  $f_{fc}$  is fuel cost for the fuel cell (\$/h),  $P_{fc}$  is fuel cell output (electrical) power (kW),  $\eta_{fc}$  is the fuel cell efficiency,  $c_{fc}$  is fuel (natural gas) price to supply the fuel cell (\$/kWh). The fuel cell efficiency can be expressed as the ratio of actual operating voltage  $V$  and 1.482 (V) [26]:

$$\eta_{fc} = V / 1.482. \quad (25)$$

In this paper the Proton Exchange membrane (PEM) fuel cell has been considered. The actual operating voltage of the fuel cell is a function of power level, and can be calculated using the following formula [26]:

$$V = \frac{1}{2} \left[ V_0 + \sqrt{V_0^2 - 4(V_0 V_{Pnom} - V_{Pnom}^2)} \xi \right], \quad (26)$$

where:  $V_0$  is theoretical or thermodynamic fuel cell potential (0.9 V);  $V_{Pnom}$  is selected cell potential at nominal power (0.45 – 0.75 V);  $\xi = P_{fc} / P_{nom}$  is the power level;  $P_{nom}$  is nominal power of the fuel cell. We assume the PEM fuel cell efficiency characteristic for  $V_0 = 0.9$  V and  $V_{Pnom} = 0.6$  V. Fig. 1 shows the fuel cost curve estimated for  $P_{nom} = 300$  kW and  $c_{fc} = 0.05$  \$/kWh.

### 3.3 Microturbine

The microturbine fuel costs  $f_{mt}$  [\$/h] can be calculated as [5]:

$$f_{mt} = c_{mt} P_{mt} / \eta_{mt}, \quad (27)$$

where  $P_{mt}$  is the microturbine electrical power output [kW],  $\eta_{mt}$  is the microturbine electric efficiency,  $c_{mt}$  is the fuel price to supply the microturbine [\$/kWh]. The efficiency of the microturbine increases with the increase of the output power [27]. The electric efficiency characteristic of the microturbine can be estimated as a quadratic function of its power output:

$$\eta_{mt} = a + bP_{mt} + cP_{mt}^2. \quad (28)$$

From a typical electrical efficiency curve of a 300 kW CGT301-302 microturbine [27] we obtain the microturbine fuel costs curve given in Fig. 1. It is assumed that the fuel price to supply the microturbine is  $c_{mt} = 0.05$  \$/kWh.

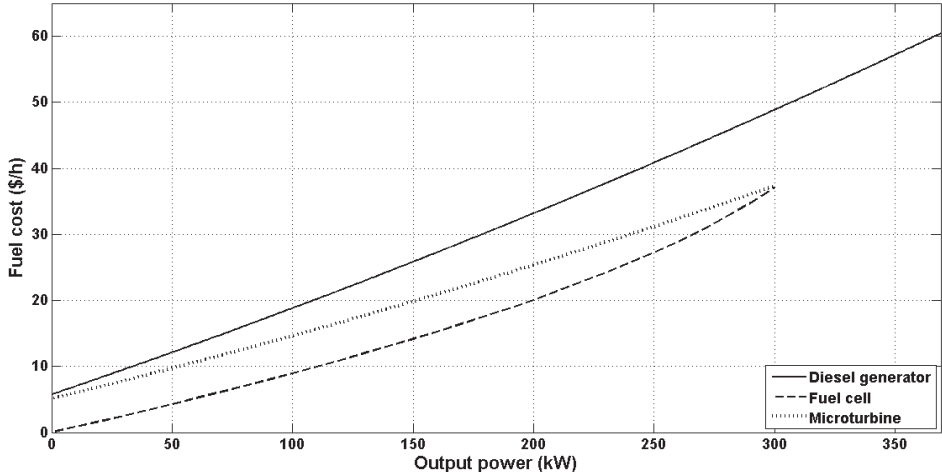


**Fig. 1 – Fuel cost characteristics of the DG units.**

### 3.4 Wind turbine

To calculate power output of a wind turbine, two main factors must be known: the wind speed on certain location and the power curve of the wind turbine. According to [28, 29] the power curve of a wind turbine can be modeled by means of a function split into four different parts:

$$P_{wt} = \begin{cases} 0, & v \leq v_{ci}, \\ \frac{v^2 - v_{ci}^2}{v_{nom}^2 - v_{ci}^2} P_{nom}, & v_{ci} < v \leq v_{nom}, \\ P_{nom}, & v_{nom} < v \leq v_{co}, \\ 0, & v > v_{co}, \end{cases} \quad (29)$$

where  $P_{nom}$ ,  $v_{nom}$ ,  $v_{ci}$  and  $v_{co}$  are nominal power, nominal wind speed, cut-in wind speed, and cut-out wind speed of the wind turbine, respectively.  $P_{wt}$  and  $v$  are denoted power output of the wind turbine and wind speed.

In this paper, we assume Vestas V44/600 kW wind turbine model [30]. The parameters used to model the power curve obtained from the owner's manual are as follows:  $P_{nom}=600$  kW,  $v_{ci}=4$  m/s,  $v_{nom}=16$  m/s и  $v_{co}=20$  m/s. Fig. 2 shows the wind speed data used to calculate the power generated by the wind turbine generator in the deterministic OPF algorithm.

### 3.5 Photovoltaic

The power output of the photovoltaic module is dependent on the solar irradiance and ambient temperature of the site as well as the characteristics of the module itself [29]. The following equation can be used to calculate the power output of the photovoltaic module  $P_{pv}$  [31]:

$$P_{pv} = P_{STC} \frac{Is}{1000} [1 + \gamma(T_c - 25)], \quad (30)$$

where  $P_{STC}$  is photovoltaic module maximum power at Standard Test Condition (STC) (W),  $Is$  is solar irradiance on the photovoltaic module surface ( $\text{W/m}^2$ ),  $\gamma$  is photovoltaic module temperature coefficient for power ( $^\circ\text{C}^{-1}$ ),  $T_c$  is photovoltaic cell (module) temperature ( $^\circ\text{C}$ ). The photovoltaic module temperature can be calculated as a function of solar irradiance and ambient temperature based on the module's nominal operating cell temperature (NOCT). The NOCT model equation is [32, 33]:

$$T_c = T_a + \frac{Is}{800} (T_{NOCT} - 20), \quad (31)$$

where  $T_a$  is ambient temperature ( $^\circ\text{C}$ ),  $T_{NOCT}$  is nominal operating cell temperature, NOCT ( $^\circ\text{C}$ ), of the module.

We assume that Sunmodule, SW 250 mono modules are used in this paper. Their performance characteristics are:  $P_{STC} = 250$  W,  $\gamma = -0.0045$   $^\circ\text{C}^{-1}$ ,  $T_{NOCT} = 46$   $^\circ\text{C}$ . Fig. 2 shows the ambient temperature and solar irradiance data

[5] used to calculate the output power generated by the photovoltaic modules in the deterministic OPF algorithm.

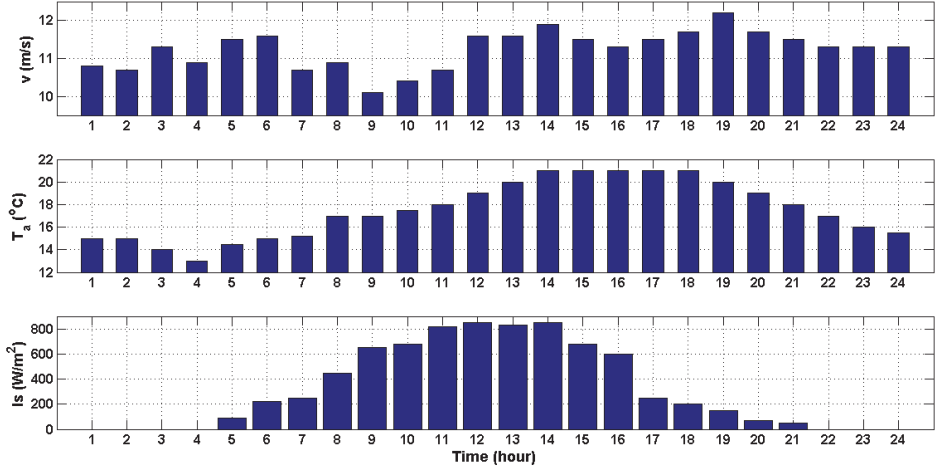


**Fig. 2 – The wind speed, ambient temperature and solar irradiance data.**

### 3.6 Electric grid

The market energy costs  $f_{gr}$  [\$/h] can be represented by quadratic function as:

$$f_{gr} = a + bP_{gr} + cP_{gr}^2, \quad (32)$$

where  $P_{gr}$  is electrical power [kW] from the electric grid and  $a, b, c$  are cost coefficients. In this paper we adopted:  $a = 0$ ,  $b = 0.1$  [\$/kWh] and  $c = 5 \cdot 10^{-5}$  [\$/ $\text{kW}^2\text{h}$ ].

## 4 Solution Method

The genetic algorithm is one of the techniques, that is, one optimization procedure based on the natural evolution process imitation [34]. They belong to the methods of a directed random search of solution domain with the aim of finding a global optimum. The classical optimization methods start from a single possible initial solution and they reach the optimum by applying the heuristic rules iteratively. The GA starts from the population, which is a group of individuals. Each individual represents a potential solution of the optimization problem. The individuals are presented in the same way, usually through a column or a string of data. The quality of each solution or individual is determined based on the fitness function values. Through a series of GA

operations a new population is obtained and its individuals are engendered by the individuals from the previous population according to the natural evolution principles: the choice of parents, crossover and mutation. Basic operations of the GA are:

1. Representation of individuals: All data (variables) that make an individual are written in a string. A string is composed of substrings. Each substring represents a binary encoded variable on which the process of optimisation is carried out. The number of substrings, therefore the size of a string, depends on the number of variables that are optimized.
2. Initialization: individuals with random strings are generated that set up the initial population.
3. Fitness function calculation: It is used to rate the quality of an individual and it represents an equivalent of the function that should be optimised, that is, objective function.
4. Selection: During the selection process the individuals that will participate in the reproduction (parents) are selected. The point of the selection is to store and transfer good individuals to the next generation.
5. Crossover: The way in which coded column parts (substrings) are crossed over actually makes a GA. Crossover is an exchange process of column parts between two individuals, that is, "parents". One or two new individuals engender by the crossover, that is, a "child". The possibility of inheriting the first parent's characteristics by a child is introduced during this process.
6. Mutation: Mutation is a way to give a new piece of information to an individual. Mutation represents an accidental bit variation of an individual, generally with a constant probability for each bit within a population. The mutation probability can further vary depending on the size of the population, application and preferences of the explorer. A fixed value which is often kept during the whole genetic algorithm is used for each generation.
7. Ending conditions: The process of finding the optimal solution by the use of the GA is an iterative process which ends when a maximum number of generations is achieved or when another criterion is fulfilled, such as a minimum offset from the best fitness value and medium fitness value of all individuals in a current population. If end conditions are fulfilled, the best individual thus obtained is the semioptimal solution in question. Otherwise, return to 3.

In this paper, the MATLAB realization of the GA is applied. The GA parameters implemented in this paper are shown in **Table 1**.

**Table 1**  
*GA Parameters.*

|                    |                                                                               |
|--------------------|-------------------------------------------------------------------------------|
| Generation         | 100                                                                           |
| Population         | 50                                                                            |
| Initial population | Feasible population                                                           |
| Selection          | Tournament, Tournament $K: 4$                                                 |
| Crossover          | Heuristic, Ratio: 1.2                                                         |
| Mutation           | Adaptive feasible                                                             |
| Ending conditions  | Max generation: 100<br>Termination tolerance on the function value: $10^{-4}$ |

## 5 Probabilistic Optimal Power Flow

When some of the input variables are uncertain, the OPF problem becomes probabilistic. Because of the probabilistic nature of wind speed and solar irradiance, the power output of the  $wt$  and the  $pv$  units are random variables as well [13]. Moreover, it is very hard to expect that the forecast of the load demand is exactly correct due to unexpected disturbance, forecast error, or load variation. Such randomly occurred factors would be the main source of uncertainties [11]. Every probabilistic formulation requires statistical characterization of the input random variables and a method for evaluating statistical features of the output variables [35].

### 5.1 Wind speed modeling

The wind speed probability density function at a certain location is generally described by a Weibull distribution [28, 29, 36, 37]:

$$f_v(v) = \frac{k}{C} \left( \frac{v}{C} \right)^{k-1} e^{-\left(\frac{v}{C}\right)^k}. \quad (35)$$

The cumulative density function (CDF) for the Weibull distribution is:

$$F_v(v) = 1 - e^{-\left(\frac{v}{C}\right)^k}. \quad (36)$$

The CDF with its inverse have been utilized to calculate the wind speed:

$$v = C(-\ln(r))^{\frac{1}{k}}, \quad (37)$$

where  $r$  are the random numbers uniformly distributed on  $[0, 1]$ . Constants  $C$  and  $k$  are the scale and shape parameters of the Weibull distribution. Different methods can be used to calculate the Weibull parameters [37]. In this paper, parameters  $k$  and  $C$  are calculated, approximately, using mean wind speed  $v_m$  and standard deviation  $\sigma$  as follows [29]:

$$k = \left( \frac{\sigma}{v_m} \right)^{-1.086}, \quad C = \frac{v_m}{\Gamma(1+1/k)}. \quad (38)$$

## 5.2 Solar irradiance modeling

Basically, the solar irradiance has stochastic nature. Therefore, probability density function should be adopted. The solar irradiance uncertainty may be characterized by normal probability density function [13, 38 – 40]:

$$f_{I_s}(I_s) = \frac{1}{\sigma\sqrt{2\pi}} e^{-\frac{(I_s-\mu)^2}{2\sigma^2}}. \quad (39)$$

Cumulative density function (CDF) for the normal distribution is:

$$F_{I_s}(I_s) = \frac{1}{2} \left[ 1 + \operatorname{erf}\left(\frac{I_s - \mu}{\sqrt{2}\sigma}\right) \right]. \quad (40)$$

CDF with its inverse have been utilized to calculate the solar irradiance:

$$I_s = \mu + \sqrt{2}\sigma \operatorname{erf}^{-1}(2r-1), \quad (41)$$

where  $r$  is a random variable having uniform distribution in  $[0, 1]$ ,  $\operatorname{erf}$  and  $\operatorname{erf}^{-1}$  are the error function and the inverse error function, respectively,  $\mu$  is hourly mean value of the solar irradiance and  $\sigma$  is standard deviation of the  $I_s$ .

Standard deviation of the hourly mean value of the solar irradiance can be pre-determined for the morning period, afternoon period and hours around the solar noon [38]. In this paper, we assume that the hourly means of solar irradiance  $\mu$  are equal to their forecasted values from Fig. 2, and values of  $\sigma$  are pre-determined with  $\sigma/\mu \cdot 100 = 8\%$  at morning (5 – 8 h) and evening hours (17 – 21 h), and 3% around the solar noon (9 – 16 h)

## 5.3 Probabilistic load model

The load is assumed to be a random variable ( $L$ ) following the same probability density function within each hour of a given daily load diagram. The PDF of the active/reactive power load will be assumed to be under the normal distribution [11, 13 – 15, 36, 41]:

$$f_L(L) = \frac{1}{\sigma\sqrt{2\pi}} e^{-\frac{(L-\mu)^2}{2\sigma^2}}, \quad (42)$$

where  $\mu$  is the mean value given as fixed load level on the daily load diagram;  $\sigma$  is standard deviation of  $L$ .

Normal CDF (43) with its inverse (44) have been used to generate the load value:

$$F_L(L) = \frac{1}{2} \left[ 1 + \operatorname{erf}\left(\frac{L - \mu}{\sqrt{2}\sigma}\right) \right], \quad (43)$$

$$L = \mu + \sqrt{2}\sigma \operatorname{erf}^{-1}(2r - 1), \quad (44)$$

where  $r$  is a random variable having uniform distribution in  $[0, 1]$ ;  $\operatorname{erf}$  and  $\operatorname{erf}^{-1}$  are the error function and the inverse error function, respectively.

In this paper it is assumed that the mean values of the active/reactive power load at each load bus are given in Fig. 4 with a standard deviation of 5%.

#### 5.4 Statistical evaluation of the output variables

Generally, the probabilistic OPF can be expressed as

$$Y = F(X), \quad (45)$$

where  $X$  is the vector of input random variables and  $Y$  is the vector of output random variables.

In the technical literature, there are several methods for evaluating the statistical features of the output variables. These methods may be classified into the three main categories: Monte Carlo simulation [41, 42], analytical methods [43, 44], and approximate methods [13, 15, 35, 45].

In this paper, an approximative method, called the point estimate method was used. The point estimate method can guarantee a great reduction of the computational efforts compared to the Monte Carlo simulation procedure [35]. This method concentrates the statistical information provided by the first few central moments of the  $m$  input random variables on  $K = 2, 3, 5$  points for each variable, named concentrations. By using these points and function  $F$ , which relates input and output variables, statistical moments of the output variables can be obtained [45]. To obtain these moments, function  $F$  has to be calculated  $2m$ ,  $2m+1$  or  $4m+1$  times depending on the adopted scheme. In this paper,  $2m+1$  scheme was used.

The  $2m+1$  scheme is more accurate than the  $2m$  scheme and performances of the  $2m+1$  and  $4m+1$  schemes are practically the same. The  $2m+1$  scheme requires  $2m+1$  evaluations of function  $F$  and uses only a two-point concentration for each input random variable [35]. Procedure for computing the moments of the output variables for the probabilistic OPF problem can be summarized by the following steps:

1. Determine number  $m$  of input random variables.
2. Set the vector of the  $j$ -th moment of the output variable equal to zero:

$$E(Y^j) = 0.$$

3. Set  $t=1$ , ( $t = 1, 2, \dots, m$ ).

4. Determine two standard locations:

$$\xi_{t,i} = \frac{\lambda_{t,3}}{2} + (-1)^{3-i} \sqrt{\lambda_{t,4} - \frac{3}{4}\lambda_{t,3}^2}, \quad i = 1, 2, \quad (46)$$

where  $\lambda_{t,3}$  is the skewness and  $\lambda_{t,4}$  is the kurtosis of the input random variable  $x_t$ .

5. Determine two locations  $x_{t,i}$

$$x_{t,i} = \mu_{x_t} + \xi_{t,i} \sigma_{x_t}, \quad i = 1, 2, \quad (47)$$

where  $\mu_{x_t}$  and  $\sigma_{x_t}$  are the mean and standard deviation of  $x_t$ , respectively.

6. Run the deterministic OPF algorithm for both locations  $x_{t,i}$  using the two input variable vectors:

$$X_i = [\mu_{x1}, \mu_{x2}, \dots, x_{t,i}, \dots, \mu_{xm}], \quad i = 1, 2, \quad (48)$$

where  $\mu_{xk}$  ( $k = 1, 2, \dots, m$  and  $k \neq t$ ) is the mean value of the remaining random input variables.

7. Determine the weight factors:

$$w_{t,i} = \frac{(-1)^{3-i}}{\xi_{t,i} (\xi_{t,1} - \xi_{t,2})}, \quad i = 1, 2. \quad (49)$$

8. Update  $E(Y^j)$ :

$$E(Y^j) = E(Y^j) + \sum_{i=1}^2 w_{t,i} [F(X_i)]^j. \quad (50)$$

9. Repeat steps 4–8 for  $t = t + 1$  until the list of random input variables is exhausted.

10. Run the deterministic OPF algorithm using as input variable vector:

$$X_\mu = [\mu_{x1}, \mu_{x2}, \dots, \mu_{x,t}, \dots, \mu_{xm}]. \quad (51)$$

11. Determine the weight factor of OPF solution of Step 10:

$$w_0 = 1 - \sum_{t=1}^m \frac{1}{\lambda_{t,4} - \lambda_{t,3}^2}. \quad (52)$$

12. Update  $E(Y^j)$ :

$$E(Y^j) = E(Y^j) + w_0 [F(X_\mu)]^j, \\ E(Y^j) = \sum_{t=1}^m \sum_{i=1}^2 w_{t,i} [F(\mu_{x_1}, \mu_{x_2}, \dots, x_{t,i}, \dots, \mu_{x_m})]^j + w_0 [F(X_\mu)]^j. \quad (53)$$

Knowing statistical moments of the output random variable, the mean and standard deviation can be computed:

$$\mu_Y = E(Y), \quad \sigma_Y = \sqrt{E(Y^2) - \mu_Y^2}. \quad (54)$$

Based on statistical moments, it is possible to approximate the probability density functions (PDFs) of the output random variables of interest using the Gram-Charlier series approach [13, 35, 43, 45].

## 6 Simulation Results

The proposed OPF approach is tested on a modified IEEE 34 node test feeder shown in Fig. 3. The original IEEE 34 node test feeder [46] is modified using assumptions given in [47]. Five different DG units were introduced in the modified test feeder. The fuel cost and output power characteristics of the DG units are given in Section 3. We assume that the DG units connected at nodes 812 (*wt*), 816 (*mt*), 854 (*pv*) and 862 (*dg*) operate in PQ mode at 0.9 power factors (produce reactive power). The DG unit at node 848 (*fc*) is capable to control active power and voltage independently, and therefore operate in PV mode. Fig. 4 shows hourly forecasted load levels in all load nodes within the distribution network.

Data for lines and nominal loads of the test feeder are reported in **Table 2**. The DG units data are listed in **Table 3**. It has a total of 9 control variables as follows: three DG unit active power outputs, one root node voltage magnitude, one PV node voltage magnitude, two voltage regulation tap settings and two shunt VAR compensator reactive power outputs. The lower and upper limits for the control variables are given in **Table 4**. The lower and upper limits of load node voltages, including DG units which are modeled as PQ nodes, are 0.95 and 1.05 p.u., respectively.

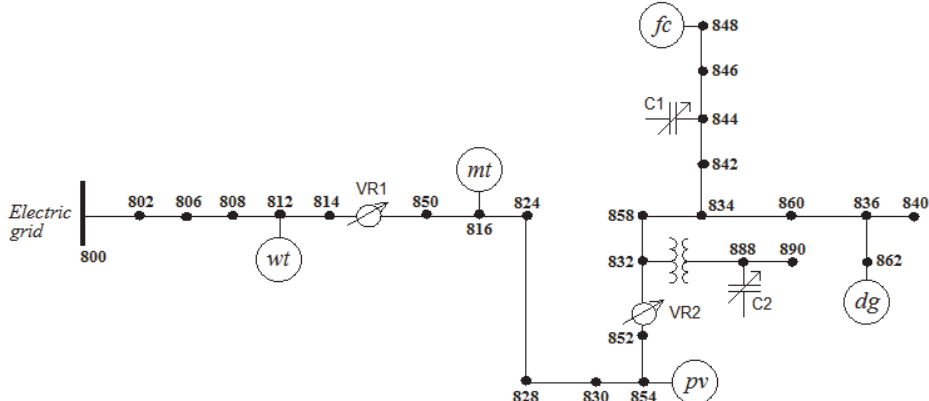


**Fig. 3 – The modified IEEE 34 node test feeder.**

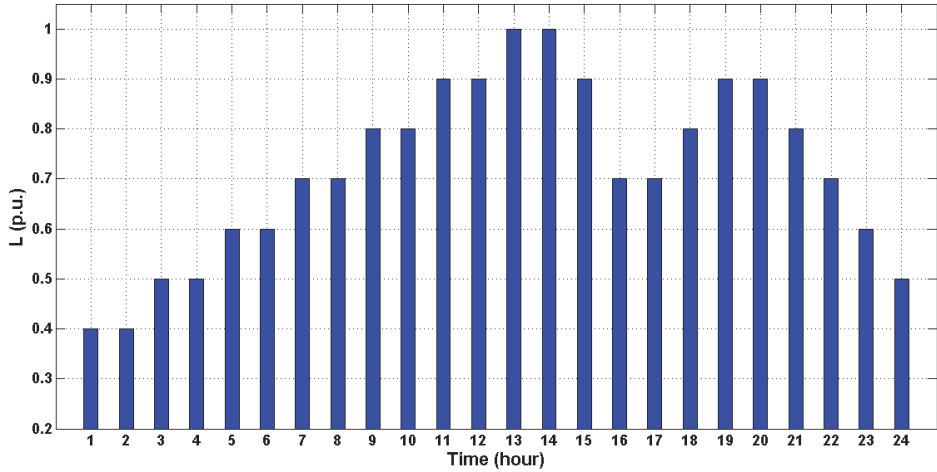


Fig. 4 – Daily load diagram in the modified IEEE 34 node test feeder.

**Table 2**  
Line data and Load data of the modified IEEE 34 node test feeder.

| Send.<br>node | Rec.<br>node | Section parameters |                  | Load at Rec. node |              |            |
|---------------|--------------|--------------------|------------------|-------------------|--------------|------------|
|               |              | $R$ [ $\Omega$ ]   | $X$ [ $\Omega$ ] | $P_L$ [kW]        | $Q_L$ [kVAr] | Load model |
| 800           | 802          | 0.5473             | 0.4072           | 27.5              | 14.5         | PQ         |
| 802           | 806          | 0.3670             | 0.2730           | 27.5              | 14.5         | PQ         |
| 806           | 808          | 6.8373             | 5.0864           | 16                | 8            | I          |
| 808           | 812          | 7.9553             | 5.9181           | 0                 | 0            | PQ         |
| 812           | 814          | 6.3069             | 4.6919           | 0                 | 0            | PQ         |
| 814           | 850          | 0.0032             | 0.0016           | 0                 | 0            | PQ         |
| 850           | 816          | 0.0992             | 0.0494           | 171.5             | 88           | PQ         |
| 816           | 824          | 3.2681             | 1.6265           | 44.5              | 22           | I          |
| 824           | 828          | 0.2689             | 0.1338           | 5.5               | 2.5          | PQ         |
| 828           | 830          | 6.5426             | 3.2562           | 48.5              | 21.5         | Z          |
| 830           | 854          | 0.1664             | 0.0828           | 4                 | 2            | PQ         |
| 854           | 852          | 11.7889            | 5.8672           | 0                 | 0            | PQ         |
| 852           | 832          | 0.0032             | 0.0016           | 7.5               | 3.5          | Z          |
| 832           | 858          | 1.5684             | 0.7806           | 25.5              | 13           | PQ         |
| 858           | 834          | 1.8661             | 0.9288           | 89                | 45           | Z          |
| 834           | 860          | 0.6466             | 0.3218           | 174               | 106          | PQ         |
| 860           | 836          | 0.8578             | 0.4269           | 61                | 31.5         | PQ         |
| 836           | 840          | 0.2753             | 0.1370           | 47                | 31           | I          |
| 836           | 862          | 0.0896             | 0.0446           | 28                | 14           | PQ         |
| 834           | 842          | 0.0896             | 0.0446           | 4.5               | 2.5          | PQ         |
| 842           | 844          | 0.4321             | 0.2151           | 432               | 329          | Z          |
| 844           | 846          | 1.1651             | 0.5799           | 34                | 17           | PQ         |
| 846           | 848          | 0.1696             | 0.0844           | 71.5              | 53.5         | PQ         |
| 832           | 888          | 11.7800            | 25.2864          | 0                 | 0            | PQ         |
| 888           | 890          | 80.2600            | 59.7059          | 450               | 225          | I          |

**Table 3**  
*DG units data in the modified IEEE 34 node test feeder.*

| Location | Type          | Mode       | $P_{Dgnom}$ [kW] | $Q_{DG}$ [kVAr] |
|----------|---------------|------------|------------------|-----------------|
| 812      | WT            | PQ         | 600              | $\cos\phi=0.9$  |
| 816      | MT            | PQ         | 300              | $\cos\phi=0.9$  |
| 854      | PV            | PQ         | 250              | $\cos\phi=0.9$  |
| 862      | DG            | PQ         | 369              | $\cos\phi=0.9$  |
| 848      | FC            | PV         | 300              | -200 ÷ 225      |
| 800      | Electric grid | Slack node | -                | -               |

**Table 4**  
*The limits of the control variables in the modified IEEE 34 node test feeder.*

| Control variables |  | Min  | Max  |
|-------------------|--|------|------|
| $P_{mr}$ [kW]     |  | 0    | 300  |
| $P_{fc}$ [kW]     |  | 0    | 300  |
| $P_{de}$ [kW]     |  | 0    | 369  |
| $V_{800}$ [p.u.]  |  | 0.97 | 1.05 |
| $V_{848}$ [p.u.]  |  | 0.98 | 1.05 |
| $t_{VR1}$ [p.u.]  |  | 0.90 | 1.10 |
| $t_{VR2}$ [p.u.]  |  | 0.90 | 1.10 |
| $Q_{C1}$ [kVAr]   |  | 0    | 300  |
| $Q_{C2}$ [kVAr]   |  | 0    | 300  |

## 6.1 Deterministic OPF analysis

In the deterministic OPF the output power of *wt* and *pv* units as well as the load level are equal to their specified (forecasted) values. Four optimization cases were considered. Case 1: fuel cost minimization for DG units; Case 2: simultaneous minimization of the fuel cost and power losses; Case 3: simultaneous minimization of the fuel cost and voltage deviation; Case 4: simultaneous minimization of the fuel cost, power losses and voltage deviation.

**Table 5** shows the optimal settings of the control variables and appropriate values of the fuel cost, power losses and voltage deviation for a min and max load level ( $T = 2h$  and  $T = 14h$ ). The underlined values indicate the optimum value of the fuel cost, power losses and voltage deviation in accordance with the optimization cases. Figs. 5 and 6 show voltage profiles of the above cases. As it could be seen, values of voltage at all nodes are within the allowable limits.

The optimal settings of the control variables for other load levels are determined too. Daily values of the fuel cost, energy loss and max voltage deviation in accordance with the optimal settings of control variables are shown in Fig. 7. Minimization of the fuel cost in Case 1 causes the maximum energy

loss in relation to other cases. In Case 2, the minimum energy loss is obtained, but the fuel cost and voltage deviation is increased to its maximum. In Case 3, the fuel cost increased in relation with Case 1 and decreased in relation with Case 2, as well as the energy loss decreased in relation with Case 1 and increased in relation with Case 2. Based on results in Figs. 5–7, Case 4 can be adopted as a compromise solution of the OPF problem.

**Table 5**  
*Optimal settings of control variables for a max and min load level.*

|                  | Max load (Time = 14 hour) |           |           |           | Min load (Time = 2 hour) |          |          |          |
|------------------|---------------------------|-----------|-----------|-----------|--------------------------|----------|----------|----------|
|                  | Case 1                    | Case 2    | Case 3    | Case 4    | Case 1                   | Case 2   | Case 3   | Case 4   |
| $P_{mt}$ [kW]    | 300.0                     | 300.0     | 300.0     | 292.3     | 0                        | 0        | 0        | 0        |
| $P_{fc}$ [kW]    | 261.2                     | 291.8     | 300.0     | 220.7     | 206.6                    | 220.5    | 200.3    | 220.4    |
| $P_{dg}$ [kW]    | 297.1                     | 369.0     | 368.1     | 367.3     | 54.5                     | 135.1    | 39.8     | 121.2    |
| $V_{800}$ [p.u.] | 0.9995                    | 1.0500    | 1.0007    | 1.0113    | 0.9809                   | 1.0500   | 1.0020   | 1.0007   |
| $V_{848}$ [p.u.] | 1.0498                    | 1.0490    | 1.0035    | 0.9891    | 1.0193                   | 0.9800   | 1.0048   | 1.0026   |
| $t_{VR1}$ [p.u.] | 0.9444                    | 0.9888    | 0.9920    | 0.9650    | 0.9559                   | 1.0908   | 0.9910   | 0.9939   |
| $t_{VR2}$ [p.u.] | 0.9667                    | 0.9865    | 0.9454    | 0.9528    | 1.0280                   | 0.9674   | 0.9911   | 0.9959   |
| $Q_{C1}$ [kVAr]  | 148.4                     | 115.1     | 300.0     | 296.6     | 104.5                    | 300.0    | 84.3     | 0        |
| $Q_{C2}$ [kVAr]  | 215.4                     | 300.0     | 300.0     | 267.7     | 112.3                    | 171.6    | 29.8     | 63.0     |
| F. cost [\$/h]   | 178.35535                 | 179.74873 | 179.64259 | 179.15529 | 55.54917                 | 56.62660 | 56.24209 | 57.42886 |
| Ploss [kW]       | 76.36                     | 64.35     | 68.90     | 79.12     | 13.56                    | 9.23     | 13.67    | 9.65     |
| Vol. dev. [p.u.] | 0.72517                   | 0.98017   | 0.49125   | 0.61854   | 0.46968                  | 0.82311  | 0.09751  | 0.10256  |

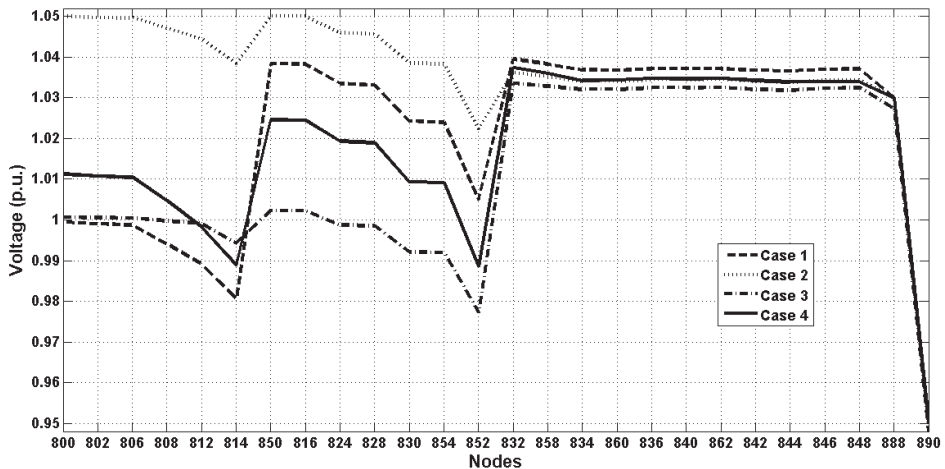


**Fig. 5 – Voltage profile for a max load level ( $T = 14$  h).**

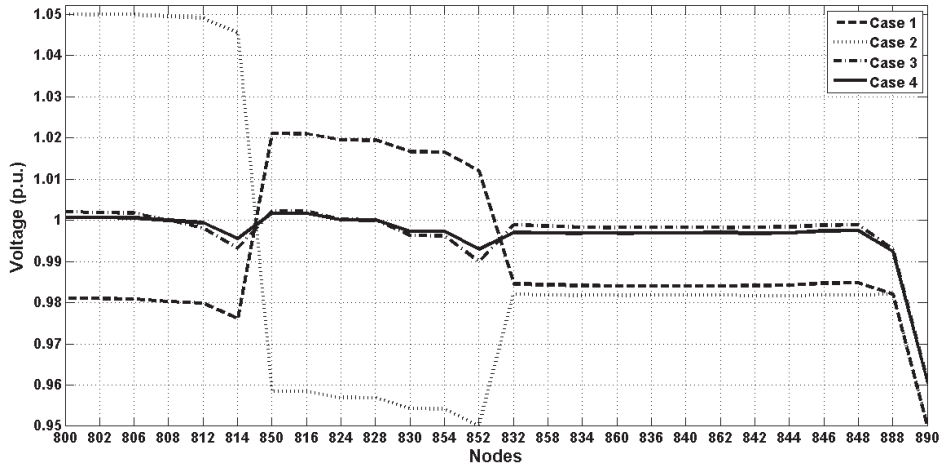


**Fig. 6 – Voltage profile for a min load level ( $T = 2$  h).**

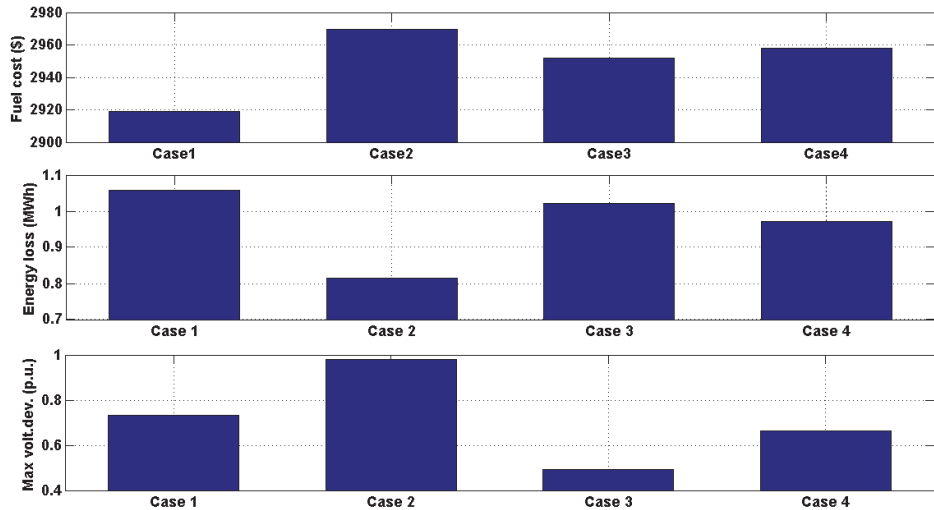


**Fig. 7 – The daily energy costs, energy losses and max voltage deviation values.**

## 6.2 Probabilistic OPF analysis

In this section, the  $wt$  and  $pv$  units power generation as well as the load level are adopted as uncorrelated input random variables. Using proper PDFs modeling for the hourly wind speed and solar irradiance given in Sections 5.1 and 5.2, the output power of  $wt$  and  $pv$  units are evaluated. All loads are fully correlated and follow the same PDF given in Section 5.3.

The  $2m+1$  point estimate method is implemented along with the GA to find the optimal solution of the probabilistic OPF. **Table 6** reports the mean and standard deviation of the OPF results. Optimization Case 1 and Case 4 were considered for Time = 14 h, 8 h and 2 h. Fig. 8 shows the PDFs of the results for optimization Case 4 and Time = 14 h. To obtain these PDFs, the Gram-Charlier expansion was used.

**Table 6**  
*Mean and standard deviation results of the probabilistic OPF.*

|                     |          | Time = 14 h |          | Time = 8 h |          | Time = 2 h |         |
|---------------------|----------|-------------|----------|------------|----------|------------|---------|
|                     |          | Case 1      | Case 4   | Case 1     | Case 4   | Case 1     | Case 4  |
| $P_{wt}$ [kW]       | $\mu$    | 297.1       | 289.3    | 271.0      | 244.7    | 58.7       | 38.7    |
|                     | $\sigma$ | 4.2         | 8.8      | 11.6       | 60.5     | 96.1       | 48.8    |
| $P_{pv}$ [kW]       | $\mu$    | 250.4       | 240.0    | 209.3      | 184.6    | 199.7      | 183.9   |
|                     | $\sigma$ | 19.9        | 17.8     | 20.5       | 47.8     | 16.0       | 20.7    |
| $P_{dg}$ [kW]       | $\mu$    | 318.9       | 317.7    | 159.5      | 145.6    | 49.2       | 101.5   |
|                     | $\sigma$ | 32.7        | 48.3     | 51.0       | 71.3     | 26.9       | 52.1    |
| $V_{800}$ [p.u.]    | $\mu$    | 1.0083      | 1.0035   | 1.0050     | 0.9960   | 0.9938     | 0.9997  |
|                     | $\sigma$ | 0.0260      | 0.0226   | 0.0180     | 0.0118   | 0.0132     | 0.0032  |
| $V_{848}$ [p.u.]    | $\mu$    | 1.0186      | 1.0073   | 1.0068     | 0.9980   | 0.9970     | 1.0046  |
|                     | $\sigma$ | 0.0166      | 0.0143   | 0.0163     | 0.0142   | 0.0036     | 0.0090  |
| $t_{VR1}$ [p.u.]    | $\mu$    | 0.9645      | 0.9621   | 0.9945     | 0.9675   | 1.0092     | 0.9975  |
|                     | $\sigma$ | 0.0273      | 0.0238   | 0.0277     | 0.0143   | 0.0111     | 0.0050  |
| $t_{VR2}$ [p.u.]    | $\mu$    | 0.9554      | 0.9548   | 0.9698     | 0.9779   | 0.9823     | 0.9952  |
|                     | $\sigma$ | 0.0152      | 0.0119   | 0.0190     | 0.0232   | 0.0116     | 0.0030  |
| $Q_{C1}$ [kVAr]     | $\mu$    | 197.8       | 231.9    | 216.1      | 196.2    | 247.5      | 178.8   |
|                     | $\sigma$ | 81.4        | 20.3     | 33.2       | 30.8     | 53.1       | 70.3    |
| $Q_{C2}$ [kVAr]     | $\mu$    | 236.8       | 254.3    | 209.8      | 209.9    | 197.3      | 181.6   |
|                     | $\sigma$ | 66.2        | 33.1     | 76.4       | 39.3     | 62.3       | 23.2    |
| F. cost [\$/h]      | $\mu$    | 178.9161    | 179.1978 | 111.9691   | 115.0566 | 55.4705    | 59.2724 |
|                     | $\sigma$ | 16.5964     | 17.1368  | 9.7492     | 10.6029  | 5.5932     | 5.5934  |
| Ploss [kW]          | $\mu$    | 77.7        | 79.2     | 38.1       | 45.4     | 13.6       | 17.5    |
|                     | $\sigma$ | 9.4         | 10.3     | 4.1        | 12.7     | 2.6        | 4.2     |
| Vol. dev.<br>[p.u.] | $\mu$    | 0.7302      | 0.6936   | 0.3603     | 0.3280   | 0.5550     | 0.0576  |
|                     | $\sigma$ | 0.1402      | 0.1380   | 0.0576     | 0.1148   | 0.0523     | 0.0075  |

In order to determine the impact of individual input random variables on the statistical characteristics of the results, we run the probabilistic OPF for five different combinations of the input random variables. Results are given in **Table 7**. From these results, it is clear that input random variable  $L$  has a higher impact on the standard deviation of the output variables than input random variables  $P_{wt}$  and  $P_{pv}$ . The reason for this is that the total power load in the distribution network is much higher than the power outputs of  $wt$  and  $pv$  units.

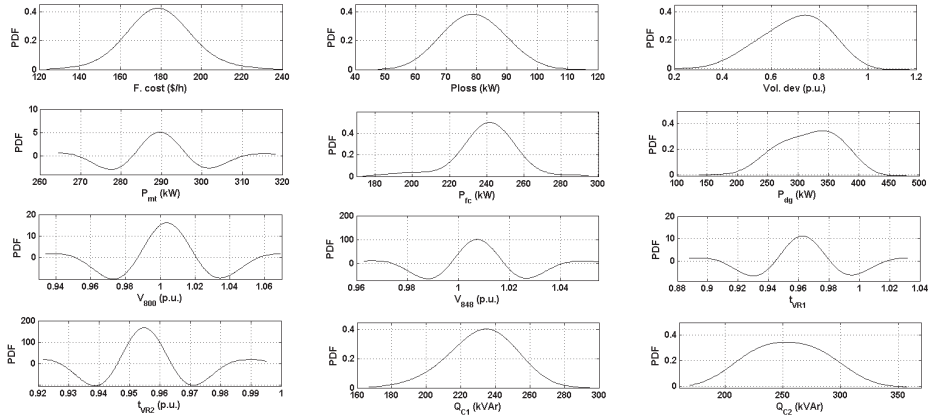


**Fig. 8 – Probability density functions of the probabilistic OPF results for Case 4 and Time = 14 h.**

**Table 7**  
Mean and standard deviation results for different combination of the input random variables.

|                     |          | Case 4, Time = 14 h<br>Input random variables |                  |          |          |          |
|---------------------|----------|-----------------------------------------------|------------------|----------|----------|----------|
|                     |          | $P_{wt}, P_{pv}, L$                           | $P_{wt}, P_{pv}$ | $P_{wt}$ | $P_{pv}$ | $L$      |
| F. cost [\$/h]      | $\mu$    | 179.1978                                      | 178.8243         | 178.8353 | 178.8601 | 179.2445 |
|                     | $\sigma$ | 17.1368                                       | 4.8933           | 4.6168   | 1.6218   | 16.4223  |
| Ploss [kW]          | $\mu$    | 79.2                                          | 76.4             | 72.7     | 75.0     | 74.0     |
|                     | $\sigma$ | 10.3                                          | 5.0              | 2.8      | 5.2      | 10.4     |
| Vol. dev.<br>[p.u.] | $\mu$    | 0.6936                                        | 0.7144           | 0.7351   | 0.6956   | 0.6955   |
|                     | $\sigma$ | 0.1380                                        | 0.0672           | 0.0458   | 0.0406   | 0.1208   |

## 7 Conclusion

In this paper, a GA based approach is proposed for the solution of the OPF in distribution networks with DG units. The OPF is formulated as a nonlinear multi-objective optimization problem with equality and inequality constraints. This formulation includes the DG units with renewable and non-renewable energy sources.

The Weibull and normal distributions are employed to model the input random variables, namely the wind speed, solar irradiance and load power. The 2m+1 point estimate method and the Gram Charlier expansion theory are used to obtain the statistical moments and the PDFs of the OPF results.

The proposed approach is examined and tested on a modified IEEE 34 node test feeder with integrated five different DG units, where several objective functions have been considered: (i) fuel cost minimization for DG units (ii) simultaneous minimization of the fuel cost and power losses (iii) simultaneous minimization of the fuel cost and voltage deviation and (iv) simultaneous minimization of the fuel cost, power losses and voltage deviation. The obtained results prove the efficiency of the proposed approach to solve both deterministic and probabilistic OPF problems for different forms of the multi-objective function. As such, it can serve as a useful decision-making supporting tool for distribution network operators and help to find out how the input random variables affect the statistical characteristics of the OPF results.

## 8 Acknowledgement

This work was supported by the Ministry of Education, Science and Technological Development of the Republic of Serbia under research grant TR 33046.

## 9 References

- [1] A.S. Safianni, G.N. Koutroumpesis, V.C. Poulos: Mixed Distributed Generation Technologies in a Medium Voltage Network, Electric Power Systems Research, Vol. 96, March 2013, pp. 75 – 80.
- [2] S.M. Moghaddas-Tafreshi, E. Mashhour: Distributed Generation Modeling for Power Flow Studies and a Three-phase Unbalanced Power Flow Solution for Radial Distribution Systems Considering Distribution Generation, Electric Power Systems Research, Vol. 79, No. 4, April 2009, pp. 680 – 686.
- [3] S. Li, K. Tomsovic, T. Hiyama: Load Following Functions using Distributed Energy Resources, IEEE Power Engineering Society Summer Meeting, Seattle, WA, USA, 16-20 July 2000, Vol. 3, pp. 1756 – 1761.
- [4] Y. Zhu, K. Tomsovic: Optimal Distribution Power Flow for Systems with Distributed Energy Resources, International Journal of Electrical Power and Energy Systems, Vol. 29, No. 3, March 2007, pp. 260 – 267.
- [5] F.A. Mohamed, H.N. Koivo: System Modeling and Online Optimal Management of Microgrid using Mesh Adaptive Direct Search, International Journal of Electrical Power and Energy Systems, Vol. 32, No. 5, June 2010, pp. 398 – 407.
- [6] J. Radosavljević, M. Jevtić, D. Klimenta: Optimal Seasonal Voltage Control in Rural Distribution Networks with Distributed Generators, Journal of Electrical Engineering, Vol. 61, No. 6, Dec. 2010, pp. 321 – 331.
- [7] B. Venkatesh: Optimal Power Flow in Radial Distribution Systems, 9th International Power and Energy Conference, Singapore, 27-29 Oct. 2010, pp. 18 – 21.
- [8] E. Atmaca: An Ordinal Optimization based Method for Power Distribution System Control, Electric Power Systems Research, Vol. 78, No. 4, April 2008, pp. 694 – 702.
- [9] A. Gabash, P. Li: Active-reactive Optimal Power Flow in Distribution Networks with Embedded Generation and Battery Storage, IEEE Transaction on Power Systems, Vol. 27, No. 4, Nov. 2012, pp. 2026 – 2035.

- [10] A. Borghetti: Using Mixed Integer Programming for the Volt/Var Optimization in Distribution Feeders, *Electric Power Systems Research*, Vol. 98, May 2013, pp. 39 – 50.
- [11] B.K. Jo, J.H. Han, Q. Guo, G. Jang: Probabilistic Optimal Power Flow Analysis with Undetermined Loads, *Journal of International Council on Electrical Engineering*, Vol. 2, No. 3, 2012, pp. 321 – 325.
- [12] A. Mohapatra, P.R. Bijwe, B.K. Panigrahi: Optimal Power Flow with Multiple Data Uncertainties, *Electric Power Systems Research*, Vol. 95, Feb. 2013, pp. 160 – 167.
- [13] T. Niknam, F. Golestaneh, A. Malekpour: Probabilistic Energy Operation Management of a Microgrid Containing Wind/Photovoltaic/Fuel Cell Generation and Energy Storage Devices based on Point Estimate Method and Self-adaptive Gravitational Search Algorithm, *Energy*, Vol. 43, No. 1, July 2012, pp. 427 – 437.
- [14] H. Ahmadi, H. Ghasemi: Probabilistic Optimal Power Flow Incorporating Wind Power using Point Estimate Method, 10th International Conference on Environment and Electrical Engineering, Rome, Italy, 08-11 ay 2011, pp. 1 – 5.
- [15] G. Verbić, C.A. Canizares: Probabilistic Optimal Power Flow in Electricity Markets based on a Two-point Estimate Method, *IEEE Transaction on Power Systems*, Vol. 21, No. 4, Nov. 2006, pp. 1883 – 1893.
- [16] O. Alsac, B. Stott: Optimal Load Flow with Steady-state Security, *IEEE Transaction on Power Apparatus and Systems*, Vol. PAS-93, No. 3, May 1974, pp. 745 – 751.
- [17] L.L. Lai, J.T. Ma, R. Yokoyama, M. Zhao: Improved Genetic Algorithms for Optimal Power Flow under Both Normal and Contingent Operation States, *International Journal of Electrical Power and Energy Systems*, Vol. 19, No. 5, June 1997, pp. 287 – 292.
- [18] A.G. Bakirtzis, P. Biskas, C.E. Zoumas, V. Petridis: Optimal Power Flow by Enhanced Genetic Algorithm, *IEEE Transaction on Power Systems*, Vol. 17, No. 2, May 2002, pp. 229 – 236.
- [19] A.A. Abou El Ela, M.A. Abido, S.R. Spea: Optimal Power Flow using Differential Evolution Algorithm, *Electrical Engineering*, Vol. 91, No. 2, Aug. 2009, pp. 69 – 78.
- [20] M.S. Kumari, S. Maheswarapu: Enhanced Genetic Algorithm based Computation Technique for Multi-objective Optimal Power Flow Solution, *International Journal of Electrical Power and Energy Systems*, Vol. 32, No. 6, July 2010, pp. 736 – 742.
- [21] S. Duman, U. Guvenc, Y. Sonmez, N. Yorukeren: Optimal Power Flow using Gravitational Search Algorithm, *Energy Conversion and Management*, Vol. 59, July 2012, pp. 86 – 95.
- [22] C.S. Cheng, D. Shirmohammadi: A Three-phase Power Flow Method for Real-time Distribution System Analysis, *IEEE Transaction on Power Systems*, Vol. 10, No. 2, May 1995, pp. 671 – 679.
- [23] S. Khushalani, J.M. Solanki, N.N. Schulz: Development of Three-phase Unbalanced Power Flow using PV and PQ Models for Distributed Generation and Study of the Impact of DG Models, *IEEE Transaction on Power Systems*, Vol. 22, No. 3, Aug. 2007, pp. 1019 – 1025.
- [24] <http://www.hardydiesel.com/john-deere-generators/dl/john-deere-generator-hdjw-225-t6.pdf>.
- [25] A.M. Azmy, I. Erlich: Online Optimal Management of PEM Fuel Cells using Neural Networks, *IEEE Transaction on Power Delivery*, Vol. 20, No. 2, April 2005, pp. 1051 – 1058.
- [26] F. Barbir, T. Gomez: Efficiency and Economics of Proton Exchange Membrane (PEM) Fuel Cells, *International Journal of Hydrogen Energy*, Vol. 22, No. 10-11, Oct/Nov. 1997, pp. 1027 – 1037.

- [27] S. Campanari, E. Macchi: Technical and Tariff Scenarios Effect on Microturbine Trigenerative Applications, Journal of Engineering for Gas Turbines and Power, Vol. 126, No. 3, Aug. 2004, pp. 581 – 589.
- [28] D. Villanueva, J.L. Pazos, A. Feijo: Probabilistic Load Flow Including Wind Power Generation, IEEE Transaction on Power Systems, Vol. 26, No. 3, Aug. 2011, pp. 1659 – 1667.
- [29] Y.M. Atwa, E.F. El-Saadany, M.M.A. Salama, R. Seethapathy, M. Assam, S. Counti: Adequacy Evaluation of Distribution System Including Wind/Solar DG During Different Modes of Operation, IEEE Transaction on Power Systems, Vol. 26, No. 4, Nov. 2011. pp. 1945 – 1952.
- [30] [http://www.windturbines.ca/vestas\\_v44.htm](http://www.windturbines.ca/vestas_v44.htm).
- [31] G.N. Tiwari, S. Dubey: Fundamentals of Photovoltaic Modules and Their Applications, RSC Publishing, Cambridge, UK, 2010.
- [32] Design Qualification Type Approval of Commercial PV Modules, IEC 61215 10.6 Performance at NOCT with IEC 60904-3 Reference Solar Spectral Irradiance Distribution, 2005.
- [33] J. Oh: Building Applied and Back Insulated Photovoltaic Modules: Thermal Models, Master Thesis, Arizona State University, Tempe, AZ, USA, Dec. 2010.
- [34] K. Y. Lee, M.A. El-Sharkawi: Tutorial on Modern Heuristic Optimization Techniques with Applications to Power Systems, IEEE Power Engineering Society, 2002.
- [35] P. Caramia, G. Carpinelli, P. Varilone: Point Estimate Schemes for Probabilistic Three-phase Load Flow, Electric Power Systems Research, Vol. 80, No. 2, Feb. 2010, pp. 168 – 175.
- [36] J.G. Vlachogiannis: Probabilistic Constrained Load Flow Considering Integration of Wind Power Generation and Electric Vehicles, IEEE Transaction on Power Systems, Vol. 24, No. 4, Nov. 2009, pp. 1808 – 1817.
- [37] S. Rehman, T.O. Halawani, T. Husain: Weibull Parameters for Wind Speed Distribution in Saudi Arabia, Solar Energy, Vol. 53, No. 6, Dec. 1994, pp. 473 – 479.
- [38] S. Kaplanis, E. Kaplanis: A Model to Predict Expected Mean and Stochastic Hourly Global Solar Radiation  $I(h; nj)$  Values, Renewable Energy, Vol. 32, No. 8, July 2007, pp. 1414 – 1425.
- [39] W.B. Wan Nik, M.Z. Ibrahim, K.B. Samo, A.M. Muzathik: Monthly Mean Hourly Global Solar Radiation Estimation, Solar Energy, Vol. 86, No. 1, Jan. 2012, pp. 379 – 387.
- [40] D. Thevenard, S. Pelland: Estimating the Uncertainty in Long-term Photovoltaic Yield Predictions, Solar Energy, Vol. 91, May 2013, pp. 432 – 445.
- [41] S. Conti, S. Raiti: Probabilistic Load Flow using Monte Carlo Techniques for Distribution Network with Photovoltaic Generators, Solar Energy, Vol. 81, No. 12, Dec. 2007, pp. 1473 – 1481.
- [42] P. Jorgensen, J.S. Christensen, J.O. Tande: Probabilistic Load Flow Calculation using Monte Carlo Techniques For Distribution Network With Wind Turbines, 8th International Conference On Harmonics and Quality of Power, 14-18 Oct. 1998, Vol. 2, pp. 1146 – 1151.
- [43] P. Zhang, S.T. Lee: Probabilistic Load Flow Computation using the Method of Combined Cumulants and Gram-Charlier Expansion, IEEE Transaction on Power Systems, Vol. 19, No. 1, Feb. 2004, pp. 676 – 682.
- [44] F.J. Ruiz-Rodriguez, J.C. Hernandez, F. Jurado: Probabilistic Load Flow for Photovoltaic Distrubuted Generation using the Cornish-Fisher Expansion, Electric Power Systems Research, Vol. 89, Aug. 2012, pp. 129 – 138.

- [45] J.M. Morales, J.P. Ruiz: Point Estimate Schemes to Solve the Probabilistic Power Flow, IEEE Transaction on Power Systems, Vol. 22, No. 4, Nov. 2007, pp. 1594 – 1601.
- [46] Distribution Test Feeders, Available at:  
<http://www.ewh.ieee.org/soc/pes/dsacom/testfeeders/index.html>.
- [47] N. Mwakabuta, A. Sekar: Comparative Study of the IEEE 34 Node Test Feeder under Practical Simplifications, 39th North American Power Symposium, Las Cruces, NM, USA, 30 Sept. – 02 Oct. 2007, pp. 484 – 491.